High-pressure Raman scattering study of defect chalcopyrite and defect stannite ZnGa2Se4

R. Vilaplana, O. Gomis, E. Pérez-González, H. M. Ortiz, F. J. Manjón et al.

Citation: J. Appl. Phys. **113**, 233501 (2013); doi: 10.1063/1.4810854
View online: http://dx.doi.org/10.1063/1.4810854
View Table of Contents: http://jap.aip.org/resource/1/JAPIAU/v113/i23
Published by the AIP Publishing LLC.

High-pressure Raman scattering study of defect chalcopyrite and defect stannite $ZnGa_2Se_4$

R. Vilaplana,[1,a)] O. Gomis,[1] E. Pérez-González,[2] H. M. Ortiz,[3,4,b)] F. J. Manjón,[4] P. Rodríguez-Hernández,[2] A. Muñoz,[2] P. Alonso-Gutiérrez,[5] M. L. Sanjuán,[5] V. V. Ursaki,[6] and I. M. Tiginyanu[6]

[1]*Centro de Tecnologías Físicas: Acústica, Materiales y Astrofísica, MALTA Consolider Team, Universitat Politècnica de València, 46022 València, Spain*
[2]*Departamento de Física Fundamental II, Instituto de Materiales y Nanotecnología, MALTA Consolider Team, Universidad de La Laguna, 38205 Tenerife, Spain*
[3]*Proyecto Curricular Licenciatura en Física, Universidad Distrital "Fco. José de Caldas," Bogotá, Colombia*
[4]*Instituto de Diseño para la Fabricación y Producción Automatizada, MALTA Consolider Team, Universitat Politècnica de Valencia, 46022 València, Spain*
[5]*Departamento de Física de la Materia Condensada y Instituto de Ciencias de Materiales de Aragón, C.S.I.C.—Universidad de Zaragoza, 50009 Zaragoza, Spain*
[6]*Institute of Applied Physics, Academy of Sciences of Moldova, 2028 Chisinau, Moldova*

(Received 3 April 2013; accepted 28 May 2013; published online 17 June 2013)

High-pressure Raman scattering measurements have been carried out in $ZnGa_2Se_4$ for both tetragonal defect chalcopyrite and defect stannite structures. Experimental results have been compared with theoretical lattice dynamics *ab initio* calculations and confirm that both phases exhibit different Raman-active phonons with slightly different pressure dependence. A pressure-induced phase transition to a Raman-inactive phase occurs for both phases; however, the sample with defect chalcopyrite structure requires slightly higher pressures than the sample with defect stannite structure to fully transform into the Raman-inactive phase. On downstroke, the Raman-inactive phase transforms into a phase that could be attributed to a disordered zincblende structure for both original phases; however, the sample with original defect chalcopyrite structure compressed just above 20 GPa, where the transformation to the Raman-inactive phase is not completed, returns on downstroke mainly to its original structure but shows a new peak that does not correspond to the defect chalcopyrite phase. The pressure dependence of the Raman spectra with this new peak and those of the disordered zincblende phase is also reported and discussed. © *2013 AIP Publishing LLC*. [http://dx.doi.org/10.1063/1.4810854]

I. INTRODUCTION

Zinc digallium selenide ($ZnGa_2Se_4$) is a tetrahedrally coordinated semiconductor of the adamantine-type $A^{II}B_2^{III}X_4^{VI}$ family of ordered-vacancy compounds (OVCs). The lack of cubic symmetry provides special properties to this family of semiconductors with important applications in optoelectronics, solar cells, and non-linear optics that has been considerably reviewed.[1–4] In particular, $ZnGa_2Se_4$ has a high photosensitivity and strong luminescence,[2] can be used for phase change memories,[5] and has been proposed as a candidate for electronic device applications forming part of heterojunction diodes.[6]

The properties of $ZnGa_2Se_4$ have been characterized by x-ray diffraction (XRD),[7,8] neutron and electron diffraction,[9–12] extended x-ray absorption fine structure,[13] infrared (IR),[14,15] Raman spectroscopy,[15–24] and magnetic[25] measurements. To this respect, while some authors claim that $ZnGa_2Se_4$ crystallizes in the tetragonal ordered defect chalcopyrite (DC) structure with space group (SG) I–4 [see Fig. 1(a)] where cations and vacancies are completely ordered,[7,13,15,16,22] other authors report that $ZnGa_2Se_4$ crystallizes in the partially disordered tetragonal defect stannite (DS) structure, also known as defect famatinite, with SG I–42 m and higher symmetry than the DC phase[8–12,21,26] [see Fig. 1(b)]. In this compound, Zn and Ga atoms have similar x-ray scattering factors and both SG I–4 and I–42 m have the same crystallographic extinctions. Therefore, the structure of $ZnGa_2Se_4$ at ambient conditions is difficult to identify by XRD so neutron scattering measurements are more suitable to determine its crystalline structure. However, the main reason to this discrepancy seems to be related to the growth process and the annealing treatment of the sample since phase diagram studies reveal that several order–disorder transitions at relatively low temperatures are present in $ZnGa_2Se_4$.[16,25,27] It is also well known that details of crystal growth and sample preparation, like the maximum temperature reached in the post-growth annealing treatment and the rate of decrease of temperature during the growth process, are crucial to understand the final structure of this compound at ambient conditions (see Refs. 24 and 25). To this respect, we have shown in a recent work[28] that DC-$ZnGa_2Se_4$ can be grown from original DS-$ZnGa_2Se_4$ by a thermal annealing at 400 °C during 10 h followed by a slow cooling to ambient temperature at a rate of 1 °C/min. In fact, the DC sample we use in the present study is obtained from DS-$ZnGa_2Se_4$ in the way described in Ref. 28.

[a)]Author to whom correspondence should be addressed. Electronic mail: rovilap@fis.upv.es
[b)]On leave from CINVESTAV, Departamento de Nanociencia y Nanotecnología (Zacatenco, México D.F.), Unidad de Querétaro, Querétaro, Mexico.

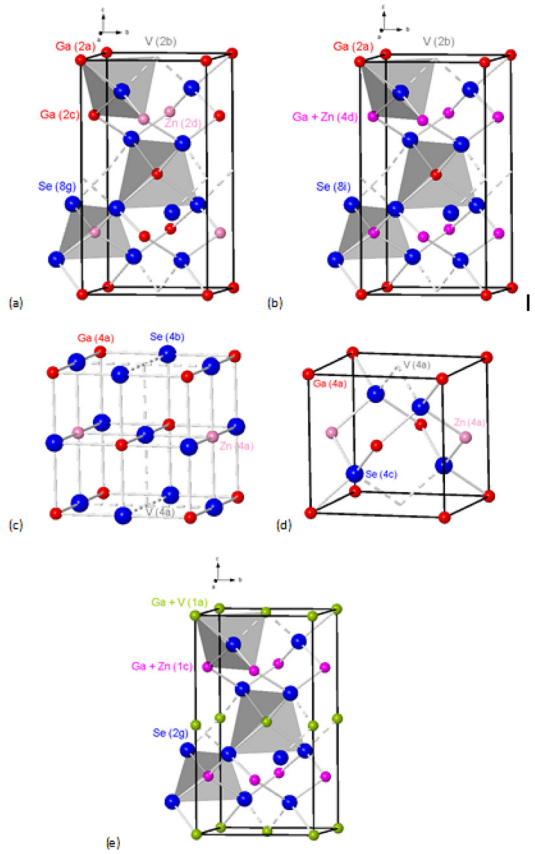

FIG. 1. $ZnGa_2Se_4$ in different structures: (a) Ordered defect chalcopyrite (DC) (model 1 in Ref. 34), (b) partially disordered defect stannite (DS) (model 6 in Ref. 34), (c) DR, (d) DZ, (e) Layered DCA (model 6 in Ref. 34). Big (blue) atoms are Se, small (red) dark atoms are Ga, and small (magenta) light atoms are Zn. Mixed Ga and Zn atoms in DS and DCA structures are shown in rose color. Mixed Ga atoms and vacancies are shown in green color. For the sake of clarity Wyckoff sites are given in parenthesis.

The influence of pressure upon the degree of disorder in the cation sublattice of $ZnGa_2Se_4$ has been discussed by various authors.[8,21,22] In Ref. 8, it was shown that DS-$ZnGa_2Se_4$ undergoes a phase transition to a sixfold-coordinated disordered rocksalt (DR) by high-pressure (HP) XRD measurements. In Ref. 21, HP Raman scattering measurements carried out in DS-$ZnGa_2Se_4$ samples evidenced a phase transition to a Raman-inactive phase that was attributed to the DR phase. A similar HP Raman study was claimed to be conducted for DC-$ZnGa_2Se_4$ samples in Ref. 22; however, we have recently commented in Ref. 28 that the samples studied in Ref. 22 are too disordered to correspond to the DC phase. Therefore, to our knowledge, there is no study of the effect of pressure on the lattice dynamics of DC-$ZnGa_2Se_4$.

In the DR phase, cations and vacancies are randomly distributed at 4*a* Wyckoff sites while anions are located at 4*b* Wyckoff sites [see Fig. 1(c)]. However, according to previous thermal theoretical predictions, the disorder process leading from the DC to the DR structure should occur in two stages.[3] In the first one, cation exchange occurs only among the initially occupied cationic sites (2*b* sites are still vacant). In the second one, the vacancies at 2*b* sites are also involved in the disorder process and the compound adopts a disordered zincblende (DZ) structure [see Fig. 1(d)] before reaching the HP-DR structure. However, the presence of two stages of disorder in OVCs at HP has been recently questioned on the basis of both theoretical and experimental studies.[29–33] To this respect, in a recent work, we studied the different possible intermediate phases of partial disorder between the initial DC or DS phases and the DZ structure and discuss the possibility to find them by means of *in situ* vibrational spectroscopy.[34]

In order to shed light on the pressure dependence of the Raman modes in DC- and DS-$ZnGa_2Se_4$ and study how pressure affects order-disorder transitions in both phases, we report here HP Raman scattering measurements at room temperature (RT) for both DC and DS structures. Note that the DC sample is completely ordered but not the DS sample which has a cationic disorder [see Figs. 1(a) and 1(b)]. We have carried out two pressure cycles (up and down) that have allowed us to follow the different pressure-induced phase transitions. We have also compared our experimental results for the 1st upstroke with theoretical calculations for both DC and DS phases and with previous HP Raman scattering measurements.[15,16,21,22] Two runs were carried out for the DC sample in order to show that the DC sample requires slightly higher pressures than the DS sample to fully transform into the Raman-inactive HP structure, tentatively attributed to the DR phase. On downstroke, the DR phase undergoes a phase transition to the DZ phase; however, the decompression of the DC sample under not complete transition to the DR phase shows a new peak apart from those of the DC phase so we speculate that the new peak could be related to the presence of a new phase, likely the layered Disordered CuAu-like (DCA) phase, on the basis of its pressure dependence and on the comparison with reported Raman spectra of disordered chalcopyrites. The technical aspects of the experiments and calculations are described in Secs. II and III. The results are presented and discussed in Sec. IV. Finally, we present the conclusions of this work in Sec. V.

II. EXPERIMENTAL DETAILS

DS-$ZnGa_2Se_4$ crystals were grown from its constituents ZnSe and Ga_2Se_3 by chemical vapor transport method using iodine as a transport agent[31] and are the same used previously in Raman scattering measurements[21,28] and in a structural study under pressure by means of XRD measurements.[8] On the other hand, DC-$ZnGa_2Se_4$ crystals were obtained from DS-$ZnGa_2Se_4$ as explained previously and reported in Ref. 28.

Samples were loaded with a 4:1 methanol-ethanol mixture as pressure-transmitting medium in the 250 μm diameter hole of an Inconel gasket inside a membrane-type diamond anvil cell. The 4:1 methanol-ethanol mixture is hydrostatic up to 10 GPa,[35] but reasonably good quasi-hydrostatic conditions are satisfied up to the maximum pressure achieved in our experiments. In this respect, pressure was determined by the ruby luminescence method[36,37] and the shape and separation of the R_1 and R_2 ruby lines were checked at each pressure and neither a significant increase in width nor an overlapping of both peaks were detected up to the highest measured pressure. Furthermore, samples were small enough ($80 \times 80\ \mu m^2$ in size and $<20\ \mu$m in thickness) to prevent bridging of the sample between the two diamonds of the diamond anvil cell.

HP unpolarized Raman scattering measurements at RT were performed in samples with incidence along the (111) pseudocubic direction, which is the usual direction of crystal growth. Raman measurements were performed with a LabRAM HR UV microspectrometer coupled to a Peltier-cooled CCD camera and using a 632.81 nm (1.96 eV) HeNe laser excitation line with a power smaller than 10 mW and a spectral resolution better than 2 cm^{-1}. During Raman experiments, samples were checked before and after each measurement in order to be sure that no heating effects occur during the measurements by the incoming laser excitation. In order to analyze the Raman spectra under pressure, Raman peaks have been fitted to Voigt profiles (Lorentzian profile convoluted by a Gaussian profile) where the spectrometer resolution is taken as the fixed Gaussian width. As already commented, two HP runs were performed in DC-$ZnGa_2Se_4$ to show that both DC and DS samples do not have the same phase transition pressure.

III. *AB INITIO* CALCULATIONS

Total-energy calculations were performed within the framework of the density functional theory (DFT) and the pseudopotential method using the Vienna *ab initio* simulation package (VASP) of which a detailed account can be found in Ref. 38 and references therein. The exchange and correlation energy has been taken in the generalized gradient approximation (GGA) according to Perdew-Burke-Ernzerhof (PBE) prescription.[39] Details of total-energy calculations in the DC structure can be consulted in Refs. 33 and 40, a plane wave cutoff of 520 eV and a k-mesh of (4 4 4) was used with the primitive cell. Total-energy calculations were also performed for the ordered DS structure of OVCs. The properties of this ordered DS phase are detailed in Refs. 15, 33, 34, and 41 and the justification about why calculations for the DS phase were performed for this ordered DS phase was already discussed in Ref. 28.

Zone-center (Γ) phonons at different pressures were calculated in the framework of Density Functional Perturbation Theory (DFPT)[42] with the Quantum Espresso package.[43] We used this code because it yields transversal optic (TO) frequencies similar to those obtained with the direct method[44] but it is much easier to calculate the longitudinal optic (LO)-TO splitting at the Γ point as explained in Ref. 28. In this way, we have calculated the TO and LO splitting of the pure polar B and E (B_2 and E) modes of the DC (DS) structure. For the lattice dynamics calculations, we have used ultrasoft pseudopotentials with an energy cutoff of 60 Ry and a k-mesh of (4 4 4) in order to obtain well converged results. Furthermore, we have used the same exchange correlation prescription as in the total-energy calculations.

IV. RESULTS AND DISCUSSION

A. First upstroke

Similarities and differences of the Raman scattering spectra of both DC- and DS-$ZnGa_2Se_4$ samples at ambient conditions were recently discussed in Ref. 28. Therefore, hereafter we will report HP Raman scattering measurements at RT and discuss the pressure dependence of the Raman modes in both DC- and DS-$ZnGa_2Se_4$ and their pressure-induced phase transitions.

According to group theory,[45] the ordered DC structure of $ZnGa_2Se_4$ (model 1 in Ref. 34) has 13 optical Raman-active modes at Γ ($3A \oplus 5B \oplus 5E$) where A modes are non-polar modes, and B and E modes are polar modes, with E modes being doubly degenerate. On the other hand, the DS structure of $ZnGa_2Se_4$ (models 1, 2, and 6 in Ref. 34) has 12 Raman-active modes ($2A_1 \oplus 2B_1 \oplus 3B_2 \oplus 5E$), where B_2 and E are polar modes, E modes are doubly degenerate, and one A_2 mode is silent. Additionally, two modes should be observed for each B and E (B_2 and E modes) in the DC (DS) structure, due to the TO-LO splitting of the polar modes. Consequently, taking into account the TO-LO splitting, up to 23 Raman-active modes could be observed in the DC phase while 21 could be observed in the DS phase.

In order to understand the Raman scattering spectra of OVCs, it is necessary to take into account that owing to the optical uniaxial character of the DC and DS crystals one may observe not pure E, B, TO, or LO modes, but quasimodes with mixed E and B or TO and LO character depending on the scattering geometry.[28,46,47] From now on, we will note the Raman modes with a letter, a subscript, and a superscript for the sake of clarity. The letter represents the symmetry of the mode, the subscript represents the different types of modes, and the superscript numbers them.

1. HP Raman measurements in DC-$ZnGa_2Se_4$

Figure 2(a) shows unpolarized RT Raman spectra of DC-$ZnGa_2Se_4$ at different pressures up to 20.1 GPa during the 1st run. The Raman spectrum can be divided into three regions: (i) the low-frequency region below 130 cm^{-1}, (ii) the medium-frequency region between 130 and 220 cm^{-1}, and (iii) the high-frequency region above 220 cm^{-1}. We have followed the pressure dependence of 14 Raman modes under pressure. The pressure dependence of the Raman modes observed in the three regions allows us to confirm the symmetry of the different observed Raman-active modes depicted in Fig. 2(a) and discussed in Ref. 28. Our Raman spectrum for DC-$ZnGa_2Se_4$ shows similar features to those observed in previous Raman works on DC-$ZnGa_2Se_4$ (Refs. 15, 16, and 24) but do not compare well with those reported by Allakhverdiev *et al.*[22] It can be noted that at pressures above 16 GPa the intensities of all the Raman peaks decrease indicating the onset of a phase transition. The disappearance of all Raman modes at 20.1 GPa suggests that apparently a phase transition to a Raman-inactive phase, which could be tentatively attributed to a DR structure (SG Fm-3 m, No. 226, Z = 1) by analogy to the HP phase found in other OVCs by XRD measurements (e.g., DS-$ZnGa_2Se_4$ (Ref. 8)), is completed.

Figure 2(b) shows the evolution of the Raman peak frequencies as a function of pressure for DC-$ZnGa_2Se_4$ up to 19 GPa. Experimental values of the first-order Raman modes of the DC phase are represented with solid symbols. For comparison with our measurements and in order to help in the identification of the different symmetries of the Raman modes, we plotted with lines in Fig. 2(b) the theoretical pressure dependence of the Raman modes with pure A-, B-, and E-symmetry for DC-$ZnGa_2Se_4$, where TO and LO modes of both B and E polar modes are plotted with solid and dashed lines,

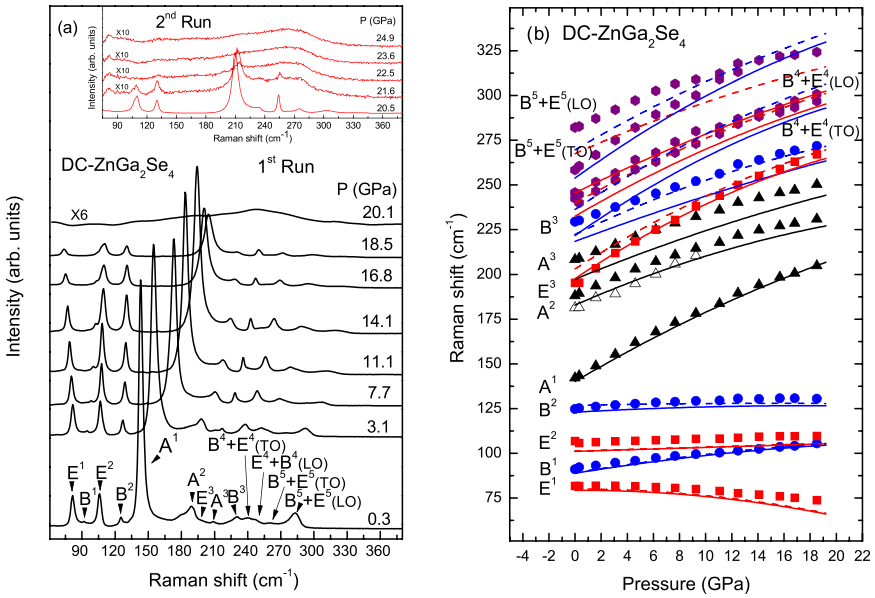

FIG. 2. (a) Unpolarized RT Raman spectra of DC-ZnGa2Se$_4$ up to 20.1 GPa carried out in the 1st run. The inset shows results from the 2nd run in DC-ZnGa2Se$_4$ from 20.5 to 24.9 GPa. (b) Pressure dependence of the experimental (symbols) and calculated (lines) vibrational modes in DC-ZnGa$_2$Se$_4$. Experimental *A*, *B*, and *E* modes are represented by solid triangles (black), solid circles (blue), and solid squares (red), respectively. Open triangles refer to the silent $A_2{}^1$ mode of DS-ZnGa$_2$Se$_4$ and the purple hexagons refer to the quasiTO and quasiLO modes with *B* and *E* mixed symmetry. Theoretical calculations for the TO (LO) phonons of pure *B* and *E* symmetry are represented by solid (dashed) lines with blue and red colors, respectively. In the case of *A* modes calculations are shown by solid black lines.

respectively. As pressure increases, the peaks in the medium- and high-frequency regions shift to higher frequencies while most of the peaks of the low-frequency region show a negligible or even negative pressure coefficient. The calculated LO-TO splittings for DC-ZnGa$_2$Se$_4$ are relatively large only for the *B* and *E* modes with the highest frequencies; i.e., the B^5 and E^5 modes and, to a lesser extent, the B^4 and E^4 modes. Table I summarizes the experimental and theoretical zero-pressure frequencies, pressure coefficients, and derivative of the pressure coefficients for the Raman modes of DC-

TABLE I. Experimental and calculated Raman frequencies in DC-ZnGa$_2$Se$_4$ at room pressure and their pressure coefficients as obtained from fits to the data using equation, $\omega = \omega_0 + aP + bP^2$, where b was multiplied by a factor 100.

Theoretical Mode (symmetry)	ω_0 (th.)[a] (cm^{-1})	a (th.)[a] ($cm^{-1}\,GPa^{-1}$)	b (th.)[a] ($cm^{-1}\,GPa^{-2}$)	Experimental mode (symmetry)	ω_0 (exp.)[b] (cm^{-1})	a (exp.)[b] ($cm^{-1}\,GPa^{-1}$)	b (exp)[b] ($cm^{-1}\,GPa^{-2}$)	ω_0 (exp.) (cm^{-1})
E^1(TO)	79.3	0.02	−3.70	E^1(TO)	82.0	−0.009	−2.40	82[c], 84[d]
E^1(LO)	80.0	0.0	−3.70	E^1(LO)				
B^1(TO)	88.9	1.18	−1.80	B^1(TO)	91.9	0.90	−0.99	92.5[c], 94[d]
B^1(LO)	89.1	1.22	−1.95	B^1(LO)				
E^2(TO)	101.0	0.22		E^2(TO)	105.8	0.28	−0.31	106[c], 109[d]
E^2(LO)	101.1	0.23		E^2(LO)				
B^2(TO)	123.0	0.41	−1.10	B^2(TO)	125.1	0.63	−1.79	126[c], 128 [d]
B^2(LO)	126.8	0.16	−0.53	B^2(LO)				129[c]
A^1	140.1	4.30	−4.33	A^1	141.9	4.53	−6.07	143[c], 145 [d]
A^2	182.8	3.20	−4.67	A^2	188.4	3.38	−5.81	182[c], 193 [d]
E^3(TO)	197.6	4.86	−7.10	E^3(TO)	194.7	5.43	−8.25	190[c]
E^3(LO)	203.1	4.69	−6.39	E^3(LO)				198[c]
A^3	197.3	3.00	−2.89	A^3	207.9	3.03	−3.99	210[c], 209 [d]
B^3(TO)	218.4	2.74	−2.06	B^3(TO)	229.2	2.77	−2.30	222[c]
B^3(LO)	222.3	3.52	−4.96	B^3(LO)				
B^4(TO)	221.7	5.12	−7.36	E^4(TO) + B^4(TO)	239.3	4.33	−6.55	233.5[c,e],235 [d]
B^4(LO)	236.3	4.83	−6.17					
E^4(TO)	232.5	4.27	−5.20	E^4(LO) + B^4(LO)	244.2	4.39	−7.55	241[c,f], 242 [d]
E^4(LO)	239.9	4.07	−4.60					248[c,f], 250 [d]
E^5(TO)	245.5	3.62	−3.42	E^5(TO) + B^5(TO)	259.0	5.30	−7.64	
E^5(LO)	267.5	3.23	−3.68					280.5[c]
B^5(TO)	253.8	5.26	−6.75	E^5(LO) + B^5(LO)	281.3	3.83	−8.05	260.5[c,g], 263 [d]
B^5(LO)	269.7	4.27	−4.60					286.5[c,g], 285 [d]

[a]Our *ab initio* calculations.
[b]Present measurements.
[c]Reference 15.
[d]Reference 16.
[e]This mode has been assigned to the TO component of the B^4 mode.
[f]These modes have been assigned to the TO and LO components of the E^4 mode.
[g]These modes have been assigned to the TO and LO components of the B^5 mode.

$ZnGa_2Se_4$. Table I also shows that our results for the Raman-active modes at zero pressure compare well with previous results reported by Eifler *et al.* and Tiginyanu *et al.* for DC-$ZnGa_2Se_4$ at ambient pressure.[15,16]

In general, a better agreement is found between the experimental and the theoretical frequencies for the Raman modes of the low- and medium-frequency region than for those of the high-frequency region. As regards the Raman modes of the low- and medium-frequency region, the agreement with calculations is remarkable and the symmetry assignment of the Raman modes in these regions is similar to that found in the literature.[15,16] A remarkable feature of the medium-frequency region is the assignment of the E^3 mode which is partially masked by close stronger A modes. We have been able to follow the pressure dependence of the E^3 mode in the DC phase and the much larger pressure coefficient measured for this mode than for those of the two close A modes is in very good agreement with our lattice dynamics calculations [see Fig. 2(b)]; thus making the assignment of this mode rather straightforward. Another curious feature of the Raman spectrum of the DC phase is the observation of a broad band at the low-frequency side of the A^2 mode whose frequency at room pressure is around 180 cm^{-1} and whose pressure coefficient is similar to that of the A^2 mode. As commented in Ref. 28, we have attributed this broad band to the local vibrations of the Se (anion) with displacements similar to those of the A^2 mode. This mode seems to be the disorder-activated silent A_2^1 mode of the DS phase and will be commented in Subsection IV A 2 when we analyze the pressure dependence of the Raman modes in DS-$ZnGa_2Se_4$. Its presence in the Raman spectrum of the DC phase indicates the presence of some remaining disorder in our DC samples.

As regards the Raman modes of the high-frequency region, we have made the symmetry assignments by comparing the Raman spectrum of DC-$ZnGa_2Se_4$ with those of other defect chalcopyrites. Our symmetry assignments are similar to those of Eifler *et al.* and Tiginyanu *et al.*[15,16] except for the high-frequency modes. Assuming that we have measured unpolarized Raman scattering with the incident and outgoing radiations along the (111) direction at all pressures, we have assigned all the modes above 230 cm^{-1} to the quasiTO and quasiLO modes resulting from the mixture of the E^4 and B^4 and of the E^5 and B^5 modes. Some of these high-frequency modes have been assigned in the previous literature as pure E and B modes. However, most of these modes should show mixed character except when measurements are performed along high symmetry directions.[28]

As commented earlier, two runs were carried out for the DC sample in order to show that this sample requires slightly higher pressures than the DS sample to fully transform into the HP DR structure. To this respect, the inset of Fig. 2(a) shows Raman spectra measured from 20.5 to 25 GPa during the upstroke of the 2nd run in one of the zones of the DC-$ZnGa_2Se_4$ crystal. It is clearly observed that the transition to the DR phase in this zone during the 2nd run occurs at a higher pressure than in the 1st run since the most intense peaks of the DC phase can be followed beyond 20.5 GPa up to 22.5 GPa. In this 2nd run, we carefully checked that all other zones of the DC-$ZnGa_2Se_4$ crystal were totally transited to the DR phase at 25 GPa.

2. HP Raman measurements of DS-$ZnGa_2Se_4$

Figure 3(a) shows RT Raman spectra of DS-$ZnGa_2Se_4$ at different pressures up to 22.0 GPa. Again, the Raman spectrum can be divided into three regions: (i) the low-frequency region below 130 cm^{-1}, (ii) the medium-frequency region between 130 and 220 cm^{-1}, and (iii) the high-frequency region above 220 cm^{-1}. We have followed the pressure dependence of 11 Raman modes under pressure. This number of Raman-active modes is comparable to those of previous measurements[21–24] and particularly agrees well with some previous works.[21,23] The symmetry of the different observed Raman-active modes is depicted in Fig. 3(a) and the pressure dependence of the Raman-active modes agrees with the symmetry assignment discussed in Ref. 28. It can be noted that above 14 GPa all Raman peak intensities decrease, thus indicating the onset of a phase transition to

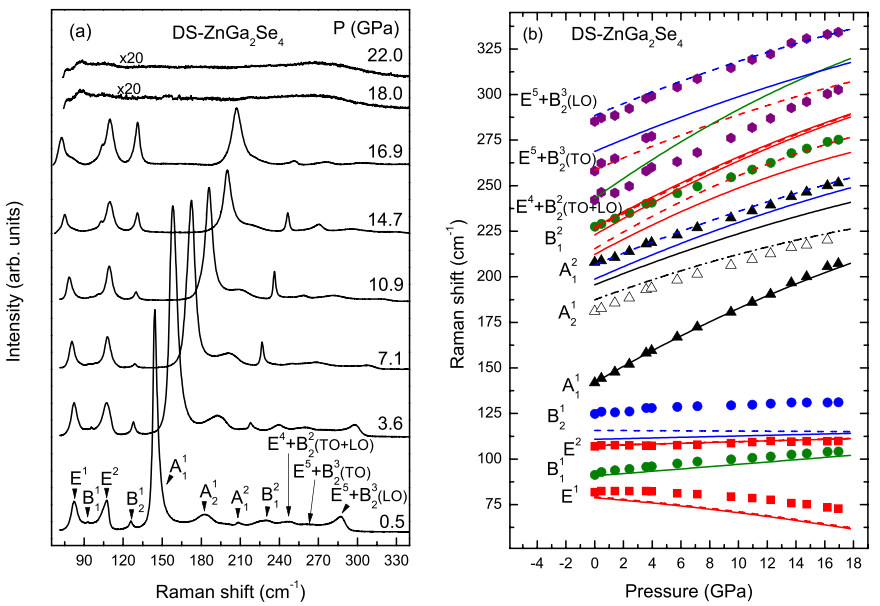

FIG. 3. (a) Unpolarized RT Raman spectra of DS-$ZnGa_2Se_4$ up to 22.0 GPa. (b) Pressure dependence of the experimental (symbols) and calculated (lines) vibrational modes in DS-$ZnGa_2Se_4$. Experimental A_1, B_1, B_2, and E modes are represented by solid triangles (black), solid circles (green), solid circles (blue), and solid squares (red), respectively. Open triangles refer to the silent A_2^1 mode and the purple hexagons refer to the quasiTO and quasiLO modes with B_2 and E mixed symmetry. Theoretical calculations for the TO (LO) phonons of pure B_2 and E symmetry are represented by solid (dashed) lines with blue and red colors, respectively. The calculations for the B_1 modes are plotted with solid green lines, and those for the A_1 and A_2 modes are plotted with solid and dashed-dotted black lines, respectively.

the Raman-inactive DR phase that seems to be completed at 18.0 GPa, in good agreement with previous HP XRD measurements on a DS-$ZnGa_2Se_4$ sample.[8]

Figure 3(b) shows the Raman mode frequencies of DS-$ZnGa_2Se_4$ as a function of pressure up to 17 GPa. Experimental values of the first-order Raman modes of the DS phase are represented with solid symbols. For comparison with our measurements and in order to help in the identification of the different symmetries of the Raman modes, we plotted with lines in Fig. 3(b) the theoretical pressure dependence of the Raman modes with pure *A*-, B_1-, B_2-, and *E*-symmetry for DS-$ZnGa_2Se_4$ using the model of the ordered DS structure as previously commented (see Ref. 28). TO and LO splittings for B_2 and *E* polar modes are noted with solid and dashed lines, respectively. Curiously, the comparison between the pressure dependence of the experimental and theoretical modes shows, in general, a rather good agreement, with the exception of the B_2^1 mode, being this agreement in the low-frequency and medium-frequency region much better than in the high-frequency region.

Table II summarizes the experimental and theoretical zero-pressure frequencies, pressure coefficients, and derivative of the pressure coefficients for the Raman modes of DS-$ZnGa_2Se_4$. Table II also shows previous results of Ursaki *et al.*[21] obtained with the same DS samples and those obtained by Alonso-Gutiérrez at ambient pressure[23] for comparison. There are several differences between our results, those of Ursaki *et al.* (apart from the different notation of the Raman modes) and those of Alonso-Gutiérrez. They were discussed previously in Ref. 28 and our experimental and theoretical pressure dependence of the Raman modes support the assignment done in Ref. 28. One of the most notable differences in the assignment of symmetry to Raman-active modes of DS-$ZnGa_2Se_4$ occurs in the medium-frequency region where a broad band around 180 cm^{-1} at ambient pressure was identified previously as the E^3 mode[21] but it was shown that this mode has *A* symmetry.[28] Fig. 3(b) shows that not only the frequency but also the pressure coefficient of this broad band are almost coincident with the expected behavior for the silent A_2^1 mode which should be absent in the Raman spectrum of the DS structure. We attribute its observation to disorder-activated Raman scattering since it is known that many silent modes become Raman active as a consequence of structural disorder.[48] In fact, in a previous work on the $Zn_{1-x}Mn_xGa_2Se_4$ series, a broad band appearing around 180 cm^{-1} in the Raman spectra of all compounds of the series, either with SG I–42 m or I–4 was assigned to disorder activated vibrations having a similar pattern as the A_2 mode.[49] Consequently, with all these considerations, we have tentatively assigned this broad band to the silent A_2^1 mode [see open triangles in Fig. 3(b)]. As mentioned previously, this mode is also present in the DC phase provided that some degree of disorder is present in the

TABLE II. Experimental and calculated Raman frequencies in DC-$ZnGa_2Se_4$ at room pressure and their pressure coefficients as obtained from fits to the data using equation, $\omega = \omega_0 + aP + bP^2$, where b was multiplied by a factor 100.

Theoretical mode (symmetry)	ω_0 (th.)[a] (cm^{-1})	a (th.)[a] (cm^{-1} GPa^{-1})	b (th.)[a] (cm^{-1} GPa^{-2})	Experimental mode (symmetry)	ω_0 (exp.)[b] (cm^{-1})	a (exp.)[b] (cm^{-1} GPa^{-1})	b (exp.)[b] (cm^{-1} GPa^{-2})	ω_0 (exp.)[c] (cm^{-1})	a (exp.)[c] (cm^{-1} GPa^{-1})	b (exp.)[c] (cm^{-1} GPa^{-2})	ω_0 (exp.)[d] (cm^{-1})
E^1(TO)	78.8	−0.64	−1.76	E^1(TO)	82.6	0.00	−3.50	84	−0.14	−2.72	84
E^1(LO)	79.3	−0.64	−1.72	E^1(LO)							
B_1^1	90.8	0.63		B_1^1	92.7	0.88	−1.20	90	1.30	−3.19	92
E^2(TO)	107.4	0.22		E^2(TO)	106.9	0.19		106	0.33	−0.31	107.2
E^2(LO)	107.4	0.22		E^2(LO)							
B_2^1(TO)	110.8	0.18		B_2^1(TO)	126	0.51	−1.20	126	0.5	−1.61	125.6[e]
B_2^1(LO)	115.7	−0.04		B_2^1(LO)							
A_1^1	142.0	4.56	−4.99	A_1^1	142.8	4.3	−2.80	143	4.38	−4.37	143.1
A_2^1	187.4	2.89	−0.33	A_2^1(silent)	182.6	2.71	−1.60	180			
A_1^2	195.6	3.14	−3.35	A_1^2	208.3	2.57		209	2.70	−2.49	207.3
B_2^2(TO)	198.7	3.49	−3.76	E^3(TO)	196			180[f]	3.10	−6.10	217.4
B_2^2(LO)	206.6	3.26	−3.21	E^3(LO)							
E^3(TO)	212.3	4.28	−6.39	B_1^2	229.3	2.76					232.6[g]
E^3(LO)	215.4	4.74	−7.36	E^4(TO) + B_2^2(TO)				243	4.34	−5.60	240
E^4(TO)	223.0	4.59	−5.35					234	1.83	−1.91	
E^4(LO)	226.3	4.33	−4.53	E^4(LO) + B_2^2(LO)	243.4	3.54		243	4.34	−5.60	247.3
E^5(TO)	227.2	4.32	−4.67					234	1.83	−1.91	
E^5(LO)	258.5	3.43	−3.97	E^5(TO) + B_2^3(TO)	260.4	4.31					265.3
B_1^2	243.0	5.60	−7.24								
B_2^3(TO)	268.8	3.34	−3.40	E^5(LO) + B_2^3(LO)	285.7	3.41	−3.00	285	3.40	−4.25	285.3
B_2^3(LO)	288.4	3.37	−3.95								

[a]Our *ab initio* calculations.
[b]Present measurements.
[c]Reference 21.
[d]Reference 23.
[e]Authors in Ref. 23 assigned this Raman peak to a B_1 mode.
[f]Authors in Ref. 21 assigned this Raman peak to the E^3 mode but it corresponds to the silent A_2^1 mode.
[g]Authors in Ref. 23 assigned this Raman peak to a B_2 mode.

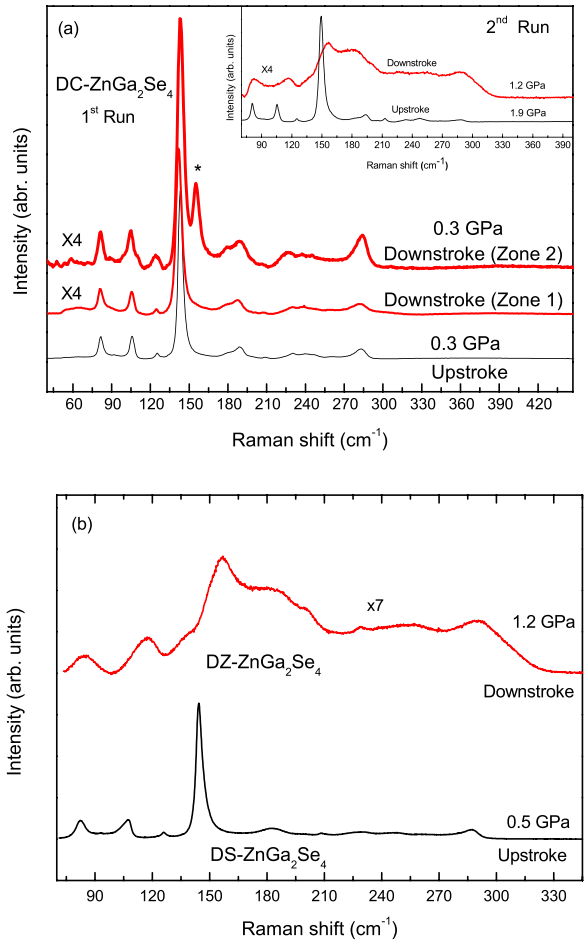

FIG. 4. (a) Raman spectra of the DS-$ZnGa_2Se_4$ crystal in the 1st upstroke at 0.5 GPa and in the 1st downstroke at 1.2 GPa with DS and DZ phase, respectively. (b) Raman spectra of the DC-$ZnGa_2Se_4$ crystal around 0.3 GPa during the 1st upstroke and during the 1st downstroke in two different zones. The inset on the top shows Raman spectra of the 2nd run of the DC-$ZnGa_2Se_4$ crystal at 1.9 GPa in the 1st upstroke and 1.2 GPa in the 1st downstroke.

DC samples. On the other hand, we have not been able to follow the pressure dependence of the weak E^3 mode (found near 196 cm^{-1} at ambient pressure[28]) and we have assigned the three modes of highest frequency (see Table II) to quasiTO and quasiLO modes having both a mixed B_2 and E character as in Refs. 23 and 28.

Finally, we have to note that both experimental and theoretical Raman frequencies in Tables I and II show a second-order pressure coefficient, b, which is consistently negative. The reason is that this pressure coefficient is related to the decrease of the compressibility of the compound with increasing pressure;[50] i.e., this coefficient is negative because of the positive value of the derivative of the bulk modulus B_0'[8] just in the same way as the first-order pressure coefficient, a, is related to the bulk modulus compressibility. In this respect it is worthy to remind that, several authors have proposed that the pressure dependence of many variables should be fitted to a modified Murnaghan equation of state.[51,52]

B. First downstroke

In this section we are going to discuss what happened to the original DS- and DC-$ZnGa_2Se_4$ samples when we decreased pressure slowly down to almost ambient pressure after upstroke in the different runs.

1. HP Raman measurements of DC sample

Fig. 4(a) shows Raman spectra on upstroke and downstroke for DC-$ZnGa_2Se_4$ at similar pressures (0.3 GPa) during the 1st run (maximum pressure 20.1 GPa). It can be observed that the Raman spectrum on recovered samples is not the same in all regions of the sample. The comparison reveals the reversibility of the DC-$ZnGa_2Se_4$ crystal in the zone 1; however, in the zone 2, there is an additional peak (marked with an asterisk) suggesting that we have possibly the initial DC phase mixed with another unknown structure or perhaps a new structure exhibiting more Raman peaks than the DC phase. A tentative nature of this new phase will be discussed later. For the moment, the result of the 1st run on DC-$ZnGa_2Se_4$ suggests that this sample could be not completely transited to the DR phase at 20.1 GPa. For this reason, as commented above, we carried out a 2nd run with a DC-$ZnGa_2Se_4$ sample but increasing the pressure till 25 GPa to be sure that the sample has entirely undergone the DC-to-DR phase transition. We checked that the phase transition to the DR phase was completed by measuring Raman spectra in different zones of the DC-$ZnGa_2Se_4$ sample because we found that the transition did not occur in all zones at the same pressure. The inset in Fig. 4(a) shows the Raman spectra measured at similar pressures on upstroke and downstroke in DC-$ZnGa_2Se_4$ crystal during the 2nd run. The broad Raman spectrum of the recovered sample looks like a one-phonon density of states, as expected for the DZ phase, and similar to that of zincblende-type ZnSe.[53] In the DZ phase, cations and vacancies are randomly distributed at 4*a* Wyckoff sites, while anions are located at 4*c* Wyckoff sites [see Fig. 1(d)]. A similar broad Raman spectrum was observed after decreasing pressure in DC-$HgGa_2S_4$ and DC-$CdGa_2Se_4$.[32,33] Therefore, we have tentatively assigned the Raman spectrum at 1.2 GPa in the downstroke to the DZ phase since this structure has been observed on downstroke in several OVCs.[54–57] We think that the Raman spectrum at 1.2 GPa on downstroke corresponds to the first-order one-phonon density of states of the DZ phase, which shows an average over the phonons of the whole Brioullin zone. The observation of the one-phonon density of states is due to the loss of translational periodicity of the lattice caused by the random distribution of the cations and vacancies at the same Wyckoff site.

2. HP Raman measurements of DS sample

Raman spectra of DS-$ZnGa_2Se_4$ obtained at 1.2 GPa on downstroke from 22.0 GPa show very broad bands and in some cases asymmetric peaks in contrast to the relatively narrow peaks measured during upstroke at a similar pressure as can be seen in Fig. 4(b). The comparison of the Raman spectra in Fig. 4(b) and the inset of Fig. 4(a) evidences that the spectrum measured on downstroke for DC-$ZnGa_2Se_4$ in the 2nd run is almost the same than that measured on downstroke for DS-$ZnGa_2Se_4$. In other words, we have observed the DZ phase on downstroke in both DC- and DS-$ZnGa_2Se_4$ samples provided that both samples undergo a complete phase transition to the DR phase. In this sense, our different

experiments show that DS-$ZnGa_2Se_4$ needs a little lower pressure to become totally transited to the DR phase than DC-$ZnGa_2Se_4$. Since the phase transition from DC or DS to DR is an order-disorder transition, the smaller pressure needed by the DS sample to complete the transition is consistent with the larger disorder already present in DS than in DC samples at ambient pressures.

C. Second upstroke

In order to know more about the nature of the new phases observed on downstroke in both DC and DS samples, we have performed Raman measurements during a 2nd upstroke.

1. HP Raman measurements of DC crystal (1st run)

Figure 5(a) shows the evolution with pressure of the Raman spectrum of the zone 2 in the recovered sample of DC-$ZnGa_2Se_4$ during the 1st run up to 22.8 GPa. We have measured the Raman spectra of zone 2 as a function of pressure because in this zone an additional strong peak appears close to the A^1 mode of the DC phase. The new peak does not correspond to the DC phase and its presence could imply, as mentioned before, mixed phases or an unknown structure with more Raman peaks than the DC phase. The new peak has a frequency at ambient pressure of 154.8 cm^{-1} and moves with a pressure coefficient of 3.3 cm^{-1} GPa^{-1}, which is slightly smaller than that of the A^1 mode of the DC structure. Note that a broad band next to the narrow A^2 mode is again observed and that the modes of the recovered DC sample in the low-frequency region are, in general, more intense than those in the high-frequency region, as in the original DC sample. As pressure increases, in general, the Raman peaks shift to higher frequencies and a general broadening of the high-frequency modes is clearly observed. At 19.2 GPa, all Raman peak intensities have decreased indicating that a phase transition to a Raman-inactive phase is taking place.

Figure 5(b) shows the Raman peak frequencies of the recovered sample (zone 2) up to 21 GPa. The solid orange diamonds refer to the new Raman mode observed. For comparison with our measurements, we plotted with lines the calculated frequencies for A, B, and E modes of the DC phase where the TO and LO modes of both B and E polar modes are plotted with solid and dashed lines, respectively. The comparison of experimental and theoretical values allows us to assign up to twelve of the theoretically predicted Raman-active modes of the DC phase. It can be observed that the evolution of the measured Raman modes during the 2nd upstroke fits reasonably well with that of the calculated DC phase.

As regards the possible nature of the new peak observed in the recovered DC sample (zone 2), its origin is not clear. However, a similar strong band was observed in chalcopyrite samples when there is a mix of chalcopyrite and layered DCA phases. Layered DCA phases are observed in epitaxial films of chalcopyrite compound and it can be viewed as layers stacked in a certain sequence.[58–60] Our Raman spectrum for DC-$ZnGa_2Se_4$ in zone 2 is very similar to the Raman spectra of the DCA phase reported for $CuInS_2$ (Ref. 58) and $CuInSe_2$,[59] where a narrow A_1 peak coming from the DCA phase is clearly observed at a slightly higher frequency than the A^1 mode of the chalcopyrite phase. To this respect, the relative intensity of these intense Raman modes has been used to estimate the relative amount of the two domains.[58,60] Moreover, several DCA phases with SG P-4m2 have been proposed to occur in ternary OVCs between the DC or DS and the DZ structures if DS phases undergo an additional disorder process involving vacancies (see Ref. 34). Figure 1(e) shows the proposed DCA phase for $ZnGa_2Se_4$ (model 6 in Ref. 34). Note that Ga atoms at 2*a* and vacancies at 2*b* sites of the DS phase get mixed to result in a structure with higher symmetry than the I-42m with cation and vacancy disorder. This DCA phase has only 6 Raman-active modes;[34] i.e., much less than the DC phase. Therefore, we tentatively propose that the additional Raman mode observed in zone 2

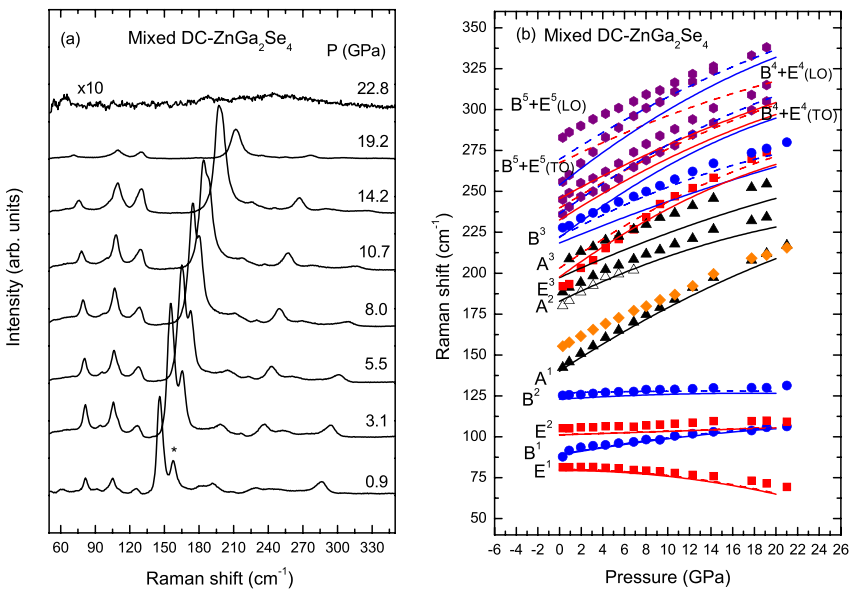

FIG. 5. (a) Raman spectra of DC-$ZnGa_2Se_4$ in zone 2 during the 2nd upstroke of the 1st run up to 22.8 GPa. (b) Pressure dependence of the experimental (symbols) and calculated (lines) vibrational modes in DC-$ZnGa_2Se_4$ during the 2nd upstroke in zone 2. Experimental A, B, and E modes are represented by full triangles (black), circles (blue), and squares (red), respectively. Open triangles refer to the silent A_2^1 mode of DS-$ZnGa_2Se_4$ and the purple hexagons refer to the quasiTO and quasiLO modes with B and E mixed symmetry. Orange diamonds refer to the new mode tentatively attributed to the A_1 mode of the DCA phase. Theoretical calculations for the TO (LO) phonons of B and E symmetry are represented by solid (dashed) lines with blue and red colors, respectively. In the case of A modes calculations are shown by solid black lines.

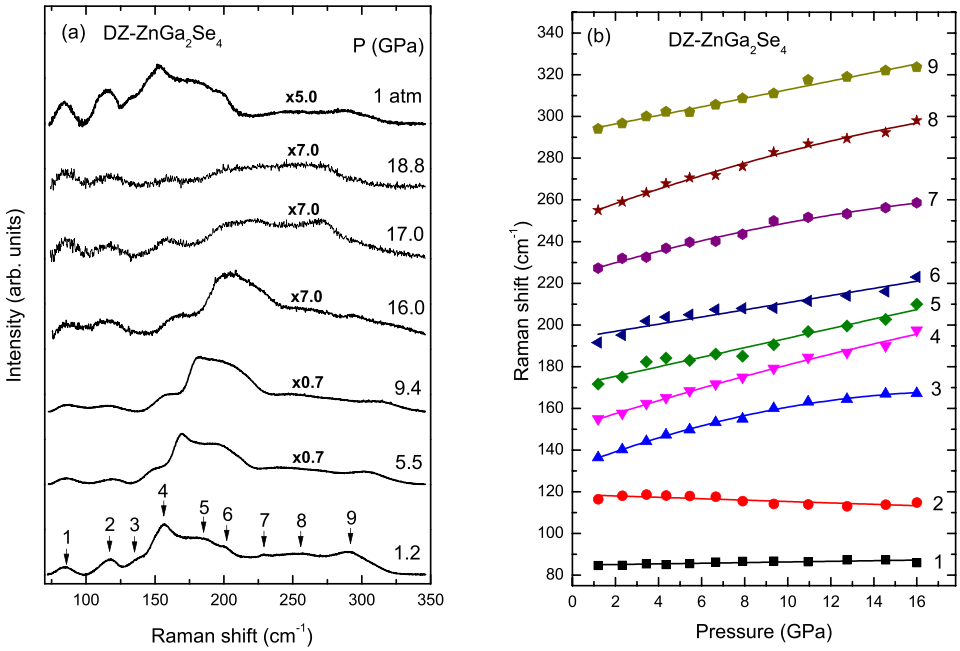

FIG. 6. (a) Room-temperature Raman spectra of DZ-$ZnGa_2Se_4$ up to 18.8 GPa during the 2nd upstroke. (b) Pressure dependence of the experimental (symbols) vibrational modes in DZ-$ZnGa_2Se_4$ during the 2nd upstroke.

of DC-$ZnGa_2Se_4$ could be an indication that the DCA phase is coexisting with the DC phase. In this respect, we note that this hypothesis needs to be confirmed by HP XRD measurements in DC-$ZnGa_2Se_4$.

2. HP Raman measurements of DS crystal

Since the DZ phase can be obtained on downstroke from both original DC and DS samples, we performed HP Raman scattering measurements only for the DZ phase obtained from the original DS sample after being pressurized to 22.0 GPa. Figure 6(a) shows selected Raman spectra of DZ-$ZnGa_2Se_4$ up to 18.8 GPa. The Raman spectrum at 1.2 GPa of DZ-$ZnGa_2Se_4$ is decomposed into several bands marked by arrows that we have followed under pressure. As pressure increases, most of the bands shift to higher frequencies and at a pressure of 17 GPa the Raman spectrum shows broad peaks of very small intensity resulting in a phase transition above 19 GPa. Since the HP phase of DZ-$ZnGa_2Se_4$ shows no significant Raman peaks and becomes opaque again, we have tentatively attributed it to the DR phase. Again, after the transition of the sample to the DR phase, we decreased slowly the pressure and found that the Raman spectrum of the released sample at ambient pressure was similar to that of a DZ phase thus confirming the reversibility of the DZ to DR phase transition.

TABLE III. Experimental Raman frequencies and pressure coefficients observed in DZ-$ZnGa_2Se_4$ as obtained from fits to the data using ($\omega = \omega_0 + aP$) or ($\omega = \omega_0 + aP + bP^2$), where b was multiplied by a factor 100.

Mode labeling	ω_0 (exp.) (cm^{-1})	a (exp.) ($cm^{-1}\,GPa^{-1}$)	b (exp.) ($cm^{-1}\,GPa^{-2}$)
1	84.8	0.15	
2	118.7	−0.33	
3	131.7	3.97	−11.00
4	151.0	3.32	−3.00
5	170.8	2.29	
6	193.5	1.72	
7	223.9	3.11	−6.00
8	250.8	3.83	−6.00
9	292.3	2.05	

Figure 6(b) shows the pressure dependence of the frequencies of the Raman bands of DZ-$ZnGa_2Se_4$ marked by arrows in Fig. 6(a). The evolution of Raman peak frequencies is practically linear with pressure with the exception of mode number 3. Table III summarizes the zero-pressure frequency, the pressure coefficient, and in some cases the derivative of the pressure coefficient of experimental Raman modes obtained from fitting the experimental data. In general, we have found that the maximum values of the pressure coefficients are smaller in the DZ phase than those in the DC and DS phases. This observation is in good agreement with HP Raman measurements of the DZ phase in $CdGa_2Se_4$ and $HgGa_2S_4$ reported in Refs. 32 and 33.

V. CONCLUSIONS

In summary, we have reported the pressure dependence of the Raman spectra of both DS- and DC-$ZnGa_2Se_4$. We have made tentative assignments of the symmetries of the different modes observed in the Raman spectra of both phases by comparing the experimental and theoretical frequencies and pressure coefficients of both phases. Our Raman measurements and calculations allow us to say that both DS and DC structures undergo an order-disorder phase transition to a Raman-inactive structure (via a single stage of disorder) that can be attributed to the sixfold-coordinated DR structure, in which cations and vacancies are completely mixed.

On decreasing pressure from the Raman-inactive phase, the samples retain the cation-vacancy disorder as expected in an irreversible order-disorder phase transition. The irreversibility of the DC to DR or DS to DR phase transitions leads to the formation of the tetrahedrally coordinated DZ phase on decreasing pressure, where all cations and vacancies are completely mixed. The partially reversible DC to DR phase

transition (in the 1st run of DC-$ZnGa_2Se_4$ up to 20.1 GPa) is a clear signature of the occurrence of an incomplete DC to DR phase transition. In this case, the initial DC structure can be recovered on decreasing pressure due to the reorganization of cations and vacancies around nucleation centers of the DC phase still not transformed to the DR phase. However, some zones of the recovered sample show an additional Raman mode which suggests that the DC phase could be mixed with another phase, whose cation-vacancy disorder is intermediate between the DC and DZ phases, and that could be tentatively attributed to the DCA phase already observed in chalcopyrites. Therefore, the results presented in this paper lead to new paths to explore other phases than those common in OVC compounds at ambient conditions.

ACKNOWLEDGMENTS

This study was supported by the Spanish government MEC under Grants No. MAT2010-21270-C04-01/03/04, by MALTA Consolider Ingenio 2010 project (CSD2007-00045), and by the Vicerrectorado de Investigación y Desarrollo of the Universitat Politècnica de València (UPV2011-0914 PAID-05-11 and UPV2011-0966 PAID-06-11). E.P.-G., A.M., and P.R.-H. acknowledge computing time provided by Red Española de Supercomputación (RES) and MALTA-Cluster.

[1]A. MacKinnon, *Tables of Numerical Data and Functional Relationships in Science and Technology*, Landolt-Börnstein New Series, Group III, Vol. 17, pt. h, edited by O. Madelung, M. Schulz, and H. Weiss, (Springer-Verlag, Berlin, 1985), p. 124.
[2]A. N. Georgobiani, S. I. Radautsan, and I. M. Tiginyanu, Fiz. Tekh. Poluprovodn. **15**, 311 (1981) [Sov. Phys. Semicond. **19**, 121 (1985)].
[3]J. E. Bernard and A. Zunger, Phys. Rev. B **37**, 6835 (1988).
[4]X. Jiang and W. R. L. Lambrecht, Phys. Rev. B **69**, 035201 (2004).
[5]I. S. Yahia, M. Fadel, G. B. Sakr, and S. S. Shenouda, J. Alloys Compd. **507**, 551 (2010).
[6]I. S. Yahia, M. Fadel, G. B. Sakr, F. Yakuphanoglu, S. S. Shenouda, and W. A. Farooq, J. Alloys Compd. **509**, 4414 (2011).
[7]H. Hahn, G. Frank, W. Klinger, A. D. Störger, and G. Störger, Z. Anorg. Allg. Chem. **279**, 241 (1955).
[8]D. Errandonea, R. S. Kumar, F. J. Manjon, V. V. Ursaki, and I. M. Tiginyanu, J. Appl. Phys. **104**, 063524 (2008).
[9]T. Hanada, F. Izumi, Y. Nakamura, O. Nittono, Q. Huang, and A. Santoro, Physica B: Condens. Matter **241–243**, 373 (1997).
[10]M. C. Morón and S. Hull, Phys. Rev. B **67**, 125208 (2003).
[11]M. C. Morón and S. Hull, J. Appl. Phys. **98**, 013904 (2005).
[12]M. C. Morón and S. Hull, J. Appl. Phys. **102**, 033919 (2007).
[13]G. Antonioli, P. P. Lottici, and C. Razzetti, Phys. Status Solidi B **152**, 39 (1989).
[14]H. Hauseler, J. Solid State Chem. **26**, 367 (1978).
[15]A. Eifler, G. Krauss, V. Riede, V. Krämer, and W. Grill, J. Phys. Chem. Solids **66**, 2052 (2005).
[16]I. M. Tiginyanu, V. V. Ursaki, and V. N. Fulga, Fiz. Tekh. Poluprovodn. **23**, 1725 (1981) [Sov. Phys. Semicond. **23**, 1069 (1989)].
[17]P. P. Lottici and C. Razzetti, Solid State Commun. **46**, 681 (1983).
[18]C. Razzetti, P. P. Lottici, and G. Antonioli, Prog. Cryst. Growth Charact. **15**, 43 (1987).
[19]G. Attolini, S. Bini, P. P. Lottici, and C. Razzetti, Cryst. Res. Technol. **27**, 685 (1992).
[20]C. Razzetti and P. P. Lottici, Jpn. J. Appl. Phys., Part 1 **32**(Suppl. 32–33), 431 (1993).
[21]V. V. Ursaki, I. I. Burkalov, I. M. Tiginyanu, Y. S. Raptis, E. Anastassakis, and A. Aneda, Phys. Rev. B **59**, 257 (1999).
[22]K. Allakhverdiev, F. Gashimzade, T. Kerimova, T. Mitani, T. Naitou, K. Matsuishi, and S. Onaric, J. Phys. Chem. Solids **64**, 1597 (2003).
[23]P. Alonso-Gutiérrez, "Estudio mediante espectroscopía Raman de la serie de semiconductores tetraédricos $Zn_{1-x}Mn_xGa_2Se_4$, Colección de Estudios de Física, Vol. 78," Ph.D. dissertation (Prensas Universitarias de Zaragoza, Zaragoza, Spain, 2009).
[24]P. Alonso-Gutiérrez, M. L. Sanjuán, and M. C. Morón, Phys. Status Solidi C **6**, 1182 (2009).
[25]D. Caldera, M. Morocoima, M. Quintero, C. Rincon, R. Casanova, and P. Grima, Solid State Commun. **151**, 212 (2011).
[26]H. Schwer, PhD dissertation, Universität Freiburg, 1990.
[27]J. C. Woolley, R. Brun del Re, and M. Quintero, Phys. Status Solidi A **159**, 361 (1997).
[28]R. Vilaplana, O. Gomis, E. Pérez-González, H. M. Ortiz, F. J. Manjón, P. Rodríguez-Hernández, A. Munóz, P. Alonso-Gutierrez, M. L. Sanjuán, V. V. Ursaki, and I. M. Tiginyanu, J. Phys.: Condens. Matter **25**, 165802 (2013).
[29]M. Fuentes-Cabrera and O. F. Sankey, J. Phys.: Condens. Matter **13**, 1669 (2001).
[30]M. Fuentes-Cabrera, J. Phys.: Condens. Matter **13**, 10117 (2001).
[31]I. M. Tiginyanu, N. A. Modovyan, and O. D. Stoika, Sov. Phys. Solid State **34**, 527 (1992).
[32]R. Vilaplana, M. Robledillo, O. Gomis, J. A. Sans, F. J. Manjón, E. Pérez-González, P. Rodríguez-Hernández, A. Muñoz, I. M. Tiginyanu, and V. V. Ursaki, J. Appl. Phys. **113**, 093512 (2013).
[33]O. Gomis, R. Vilaplana, F. J. Manjón, E. Pérez-González, J. López-Solano, P. Rodríguez-Hernández, A. Muñoz, D. Errandonea, J. Ruiz-Fuertes, A. Segura, D. Santamaría-Pérez, I. M. Tiginyanu, and V. V. Ursaki, J. Appl. Phys. **111**, 013518 (2012).
[34]F. J. Manjón, O. Gomis, R. Vilaplana, J. A. Sans, and H. M. Ortiz, Phys. Status SolIdi B DOI: 10.1002/pssb.201248596 (published online).
[35]G. J. Piermarini, S. Block, and J. D. Barnett, J. Appl. Phys. **44**, 5377 (1973).
[36]K. Syassen, High Press. Res. **28**, 75 (2008).
[37]H. K. Mao, J. Xu, and P. M. Bell, J. Geophys. Res. **91**, 4673, doi:10.1029/JB091iB05p04673 (1986).
[38]G. Kresse *et al.*, Computer code VASP, see http://www.vasp.at.
[39]J. P. Perdew, K. Burke, and M. Ernzerhof, Phys. Rev. Lett. **78**, 1396 (1997).
[40]F. J. Manjón, O. Gomis, P. Rodríguez-Hernández, E. Pérez-González, A. Muñoz, D. Errandonea, J. Ruiz-Fuertes, A. Segura, M. Fuentes-Cabrera, I. M. Tiginyanu, and V. V. Ursaki, Phys. Rev. B **81**, 195201 (2010).
[41]A. Eifler, J.-D. Hecht, G. Lippold, V. Riede, W. Grill, G. Krauss, and V. Krämer, Physica B **263–264**, 806 (1999).
[42]S. Baroni, S. Gironcoli, A. del Corso, and P. Giannozzi, Rev. Mod. Phys. **73**, 515 (2001).
[43]P. Giannozzi, S. Baroni, P. Bonini *et al.*, J. Phys.: Condens. Matter **21**, 395502 (2009).
[44]K. Parlinski, Computer code PHONON, see: http://www.computingformaterials.com/index.html.
[45]E. Kroumova, M. I. Aroyo, J. M. Perez-Mato, A. Kirov, C. Capillas, S. Ivantchev, and H. Wondratschek, Phase Transitions **76**, 155 (2003).
[46]R. Loudon, Adv. Phys. **13**, 423 (1964).
[47]P. Alonso-Gutiérrez and M. L. Sanjuán, Phys. Rev. B **78**, 045212 (2008).
[48]F. J. Manjón, B. Marí, J. Serrano, and A. H. Romero, J. Appl. Phys. **97**, 053516 (2005).
[49]P. Alonso-Gutiérrez, M. L. Sanjuán, and M. C. Morón, Physics of Semiconductors, AIP Conf. Proc. **893**, 185 (2007).
[50]M. Cardona, J. Phys. Collog. **45**, 29 (1984).
[51]M. D. Frogley, J. L. Sly, and D. J. Dunstan, Phys. Rev. B **58**, 12579 (1998).
[52]M. D. Frogley and D. J. Dunstan, Phys. Stat. Sol. (b) **211**, 17 (1999).
[53]H. Bilz and W. Kress, *Phonon Dispersion Relations in Insulators, Springer Series in Solid-State Sciences* (Springer-Verlag, Berlin, 1979), Vol. 10.
[54]A. Grzechnik, V. V. Ursaki, K. Syassen, I. Loa, I. M. Tiginyanu, and M. Hanfland, J. Solid State Chem. **160**, 205 (2001).
[55]S. Meenakshi, V. Vijyakumar, B. K. Godwal, A. Eifler, I. Orgzall, S. Tkachev, and H. D. Hochheimer, J. Phys. Chem. Solids **67**, 1660 (2006).
[56]S. Meenakshi, V. Vijyakumar, A. Eifler, and H. D. Hochheimer, J. Phys. Chem. Solids **71**, 832 (2010).
[57]O. Gomis, R. Vilaplana, F. J. Manjón, D. Santamaría-Pérez, D. Errandonea, E. Pérez-González, J. López-Solano, P. Rodríguez-Hernández, A. Muñoz, I. M. Tiginyanu, and V. V. Ursaki. MRS Bull. **48**, 2128 (2013).
[58]J. Alvarez-García, A. Pérez-Rodríguez, B. Barcones, A. Romano-Rodríguez, J. R. Morante, A. Janotti, S.-H. Wei, and R. Scheer, Appl. Phys. Lett. **80**, 562, (2002).
[59]B. J. Stanberya, S. Kincal, S. Kim, C. H. Chang, S. P. Ahrenkiel, G. Lippold, H. Neumann, T. J. Anderson, and O. D. Crisalle, J. Appl. Phys. **91**, 3598 (2002).
[60]D. S. Su and S. H. Wei, Appl. Phys. Lett. **74**, 2483 (1999).